

Application of waveform tomography at the Campos Basin field

Mauricio Pedrassi^{1*}, Jyoti Behura², Thomas L. Davis³, Esteban Diaz³ and Satyan Singh³ present the waveform inversion of the OBC Campos Basin field, defining the best parametrisation in order to obtain an improved version of the velocity model of the area.

Campos Basin field has been continuously characterised at the Reservoir Characterization Project (RCP) in Colorado School of Mines. Past research includes poststack and prestack joint inversions of PP and PS data which increased the reservoir resolution and could predict a porosity map. To further improve characterisation of the Campos Basin field, waveform tomography (WT), or full waveform inversion (FWI), is performed for a 2D line from the 2010 ocean bottom cable (OBC) data under a 2D acoustic isotropic medium assumption. The goal is to bring high resolution and accuracy to the P wave velocity model for better-quality reservoir imaging. In order to achieve the best results the application of WT to the 2D dataset required defining the suitable parameters to these data, where the main options in the inversion are the type of objective function, the time domain damping, and the frequency discretisation. Waveform inversion has improved the final velocity model, as verified by migrated images showing more continuous and focused horizons at the reservoir depth. The improved seismic image and velocity model are possible inputs, respectively, to a new geological interpretation and to acoustic/elastic attributes inversion.

Waveform tomography (WT), or Full Waveform Inversion (FWI), has been the subject of studies and conceptual development over the past 30 years (Virieux and Operto, 2009). Furthermore, research groups and the oil industry around the world have shown the improvement that WT can bring to the velocity model, especially in terms of high resolution in comparison with conventional techniques, such as traveltime tomography (TT) or migration velocity analysis (MVA). These techniques can only build a smoothed version of the velocity model, containing the kinematics of the wavefield, even though they are able to generate a good quality seismic image. WT represents a more advanced approach that attempts to completely describe the complex interaction of the propagating waves and the earth, in which the phase of the whole waveform is used in the model reconstruction (Pratt, 2013).

Although WT is not a completely developed technique yet, and has several challenges to overcome, such as the computational limits imposed by 3D-elastic modelling and the estimation of anisotropy parameters among others, WT inversions performed under feasible 2D acoustic isotropic medium assumptions can provide reasonable, high resolution, final velocity models (Sirgue and Pratt, 2004).

Improvements in the final result are highly dependent on a sufficiently accurate initial model, the minimum frequency of the data, the acquisition design (maximum offset) of the survey, and the source signature used to generate the synthetic data. All of these factors contribute to the WT convergence, potentially leading to the correct velocity model. The initial velocity model is usually obtained from TT or from MVA, which contains the background velocity information and can locate the objective function close to the global minimum. Reflection seismic data may not have low enough frequency content and large enough offsets to provide good parameters for waveform inversion success.

The Campos Basin field has been part of Reservoir Characterization Project (RCP) research for four years. The field is a deepwater turbidite sandstone, and the data for the project are provided by Petrobras S.A. To further improve characterisation of the Campos Basin field, waveform inversion is applied in this seismic data in order to obtain a higher resolution and more accurate P-wave velocity model of the area, focusing at the reservoir depth. The waveform inversion is performed using a 2D acoustic isotropic medium assumption. By improving the velocity model of the area, the updated seismic images will provide new geological interpretation as well as new attribute maps. Likewise, the updated velocity model may be incorporated in acoustic/elastic attribute inversions to better constrain the results.

Waveform tomography is a type of data matching method which attempts to recover the model parameters that best explain the observed data. Waveform Tomography is performed in the frequency domain (Pratt and Worthington, 1990), using software provided by Prof Gerhard Pratt (Pratt,

¹ *Petroleo Brasileiro S.A. – Petrobras.*

² *Seismic Science LCC.*

³ *Colorado School of Mines.*

* *Corresponding author, E-mail: mpedrass@mymail.mines.edu*

Data Processing

2013), which has proven to be efficient. This paper will present the waveform inversion of the OBC Campos Basin field, defining the best parametrisation and strategy in order to obtain an improved version of the velocity model of the area.

Waveform inversion is a non-linear inverse problem and it is solved using a linearised least square solution by minimising the objective function. The objective function is defined based on the difference between observed and modelled data. Because of the high computational costs for seismic forward modeling, instead of a global search, the minimisation is obtained by local methods. The model perturbation (δm), is obtained by the steepest descent method (the gradient) and the model parameters (m) are iteratively updated until they reach some convergence criteria.

$$m^{(k)} = m^{(k-1)} - \delta m^{(k-1)}, \delta m^{(k-1)} = -\alpha^{(k-1)} \nabla E^{(k-1)} \quad (1)$$

Data and geometry

Waveform inversion is performed for a 2D line extracted from a 3D, 4C ocean-bottom-cable survey (OBC), which was conducted in 2010 with the purpose of doing 4D analysis in the reservoir area, using the 2005 OBC survey

as baseline. The 2D dataset used in the inversion is the pressure component of the acquired field data without any type of pre-processing. It was only bandpass filtered (1Hz to 30Hz) and resampled to 4 ms. The data are composed of 347 sources with a constant interval of 43.75 m and 247 receivers 25 m equally spaced. Figure 1 shows the 2D geometry of the line, which includes wells, sources, receivers and the initial velocity model coordinates. Figure 2 shows the relative position of sources and receivers overlaid with the initial velocity model.

Waveform inversion parametrisation

Waveform inversion is a technique which requires interaction between users and data. Several tests were performed in order to understand and optimise the main parameters of the process. The definition of the objective function, the time damping parameter (data selection) and the frequency discretisation are discussed in this section.

Objective function

The objective function is based on the difference between the modelled and observed data. Since waveform tomography is applied in the frequency domain, the data have amplitude

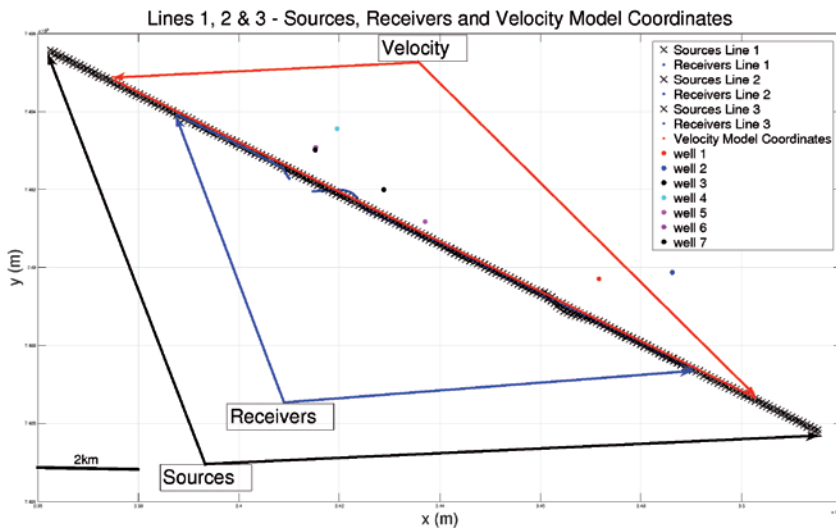


Figure 1 Geometry map which includes sources, receivers, velocity model and well coordinates.

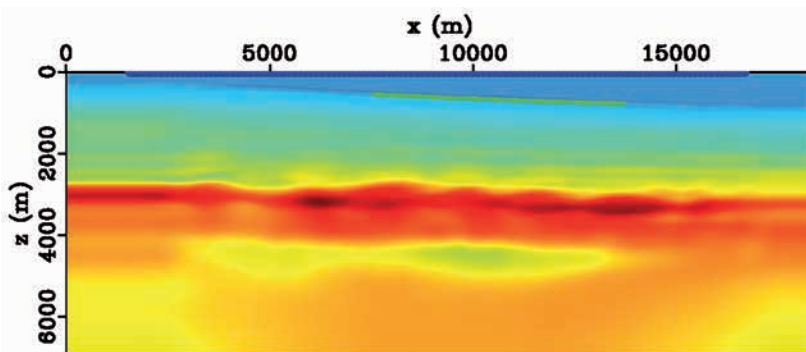


Figure 2 2D geometry configuration with sources (blue), receivers (green) and the initial velocity model overlaid. Cable length is approximately 6.2 km.

and phase parts, and the objective function can be defined using amplitude and phase together or only amplitude or only phase (Shin et al., 2007; Bednar et al., 2007; Pyun et al., 2007). Because of the inherent variation of the amplitude of the data with offset and depth, and to avoid dealing with it in the forward modelling code, it is more stable to define a phase's objective function, where the amplitude is ignored. Depending on the frequency content available in the data, the phase inversion can reconstruct a high-resolution velocity model (Alkhalifah, 2014). In fact, the objective function here is defined in the logarithmic phase-only residuals (Bednar et al., 2007).

Diving waves

Depending on the velocity gradient, diving waves travel through the earth subsurface bending back towards to the recording surface without reflecting from any sharp subsurface interface. The strategy question is: 'Why should we start or focus the inversion only on diving waves?'. The diving wave signature (the banana-shaped object) shows its effective ray path (Woodward, 1992) that directly connects the source and receiver, therefore the region where the inversion is capable of updating the velocity model, the first Fresnel zone. In contrast, the reflection signature (elliptical object – isochrone), which also describes all possible update positions in the model, does not represent the associated ray path and thus makes it difficult to locate the update in the velocity model.

The diving wave signature impels to focus the inversion on the diving waves to first update the background velocity model. The background update will be determined by the depth that diving waves can probe, and depends on the frequency content and offsets available in the data. Low frequency and larger offsets provide deeper background updates. In addition, it is not a good strategy to start the inversion including reflections since the initial velocity model is smooth and usually not accurate enough, which makes it difficult to generate reflections at the right times. The reflections can be included later in the inversion.

Focusing the inversion on diving waves and at the depth of the reservoir, the idea is to evaluate if the inversions will be able to update the velocity model at a certain depth, in our case, the depth of the reservoir, approximately 2.5 km deep. In order to verify whether or not diving waves travelled through the reservoir depth and were effectively measured at the sea floor, a ray tracing modeling and a sensitivity kernel analysis were performed using the initial velocity. Both analysis confirmed that the diving waves travelled through the reservoir and the sensitivity kernels generally showed that for lower frequencies, independent of offset, the wavefield is sensitive through the entire model, where the diving waves update (first Fresnel zone) has a limited depth extent up to approximately 2 km and reflections update reach the deeper part of the model.

Time domain damping (data selection)

The time domain damping (τ) is used in the frequency domain waveform inversion for two different purposes. First, to avoid the time-aliasing (wrap-around in time domain), however, the main reason is to select the data that will be included in the inversion process. The waveform inversion code provides different options to apply the time domain damping in the data and for simplicity in this work it was applied directly to the data at a constant start time, $t = 0$ s. It might not be the best option because it suppresses useful diving waves in the data at larger offsets.

As discussed, the waveform inversions are focusing on diving waves. In order to avoid reflections, a strong time damping can be helpful in attenuating the later arrivals. Likewise, larger offsets are more sensitive to errors in the velocity model, which means that modelled data can be generated with a time delay larger than a half cycle from the observed data – in other words, the cycle can be skipped. Non-linearity (cycle-skipping) in waveform inversion is discussed in the next section on frequency discretisation. In addition, after the background velocity model is updated by the first few inversions, reflections may be included in the inversions by relaxing the time domain damping parameter.

Frequency discretisation

Frequency discretisation is based on the approach developed by Sirgue and Pratt (2004), where they theoretically proved for the 1D model that a single frequency and a range of sources/receivers offsets $[0, x_{\max}]$ can recover a range of vertical wavenumbers $[kz_{\min}, kz_{\max}]$. Each source/receiver pair contributes a single vertical wavenumber. Furthermore, this strategy has also been shown to be capable of dealing with more complex 2D models, where the structures are nonhorizontal, the incident and scattering angles are different, and therefore a range of nonvertical wavenumbers can be recovered.

The frequency discretisation always provides a much smaller number of frequencies to be inverted when compared with the number of frequencies provided by Sampling Theorem. It is one of the biggest advantages of performing the waveform inversion in the frequency domain. Following the frequency discretisation strategy, which depends on the maximum half-offset survey ($h_{\max} = 3.0$ km) and on the depth of the target (reservoir - $z = 3.0$ km), the frequencies to be inverted are $f = 2.0, 2.8, 4.0, 5.6, 8.0, 11.3$ and 15 Hz. Since we are dealing with real data, which includes noise, three to four frequencies were added to each selected frequency which built groups of frequencies. This group approach helps to suppress the influence of noisy data with redundancy in the recovered wavenumber in each group.

In order to compute the frequencies to be inverted one needs to define the lowest reliable frequency in the data.

Data Processing

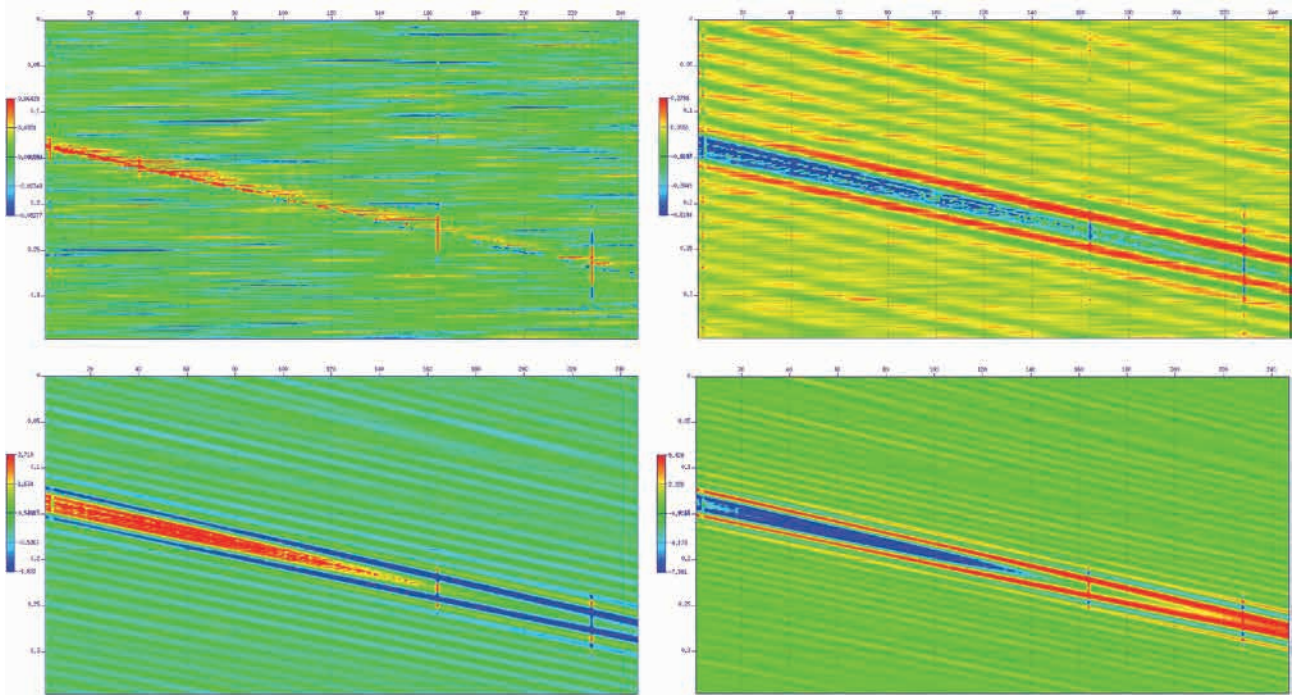


Figure 3 Amplitude of the real part of the data for four frequencies: a) top left - $f=1\text{Hz}$; b) top right - $f=2\text{Hz}$; c) bottom left - $f=3\text{Hz}$ and d) bottom right - $f=4\text{Hz}$. Each pair source/receiver is a complex number, the plots here show the real part of all pairs sources/receivers in the form $(x,z)=(\text{sources} \times \text{receivers})$.

Figure 3 shows the real part of the dataset for four different low frequencies ($f = 1, 2, 3, 4 \text{ Hz}$) which its signal to noise ratio (SNR) is visually recognisable. Each panel represents the entire data for a particular frequency, where receivers are in the x -direction and the sources are in the z -direction. Each source/receiver pair is a complex data with a real and imaginary part and in these panels the amplitude of the real part is plotted. The SNR attribute and the coherency were used to choose the lowest frequency to start the inversions.

The basin of attraction of the objective function and the half-cycle of the data increases for low frequencies. Because of this fact, the starting inversion frequency was selected as 2 Hz. The 2Hz component of the data presents a good SNR and coherency and a lowest frequency option can better help to overcome the non-linearity of the objective function. Also, the multi-scale approach is used in order to effectively overcome the non-linearity of the objective function, avoiding being trapped in local minima, where the inversion starts with the lowest frequency of the data. This data is less sensitive to the cycle-skipping issue, and sequentially inverts for higher frequencies. After each frequency inversion the velocity model is more accurate and for the next-higher frequency the modelled data will be within a half-cycle from the observed data.

Gradient preconditioning

The Newton algorithm solution includes the Hessian matrix (H), which is a type of filter that modifies the gradient direc-

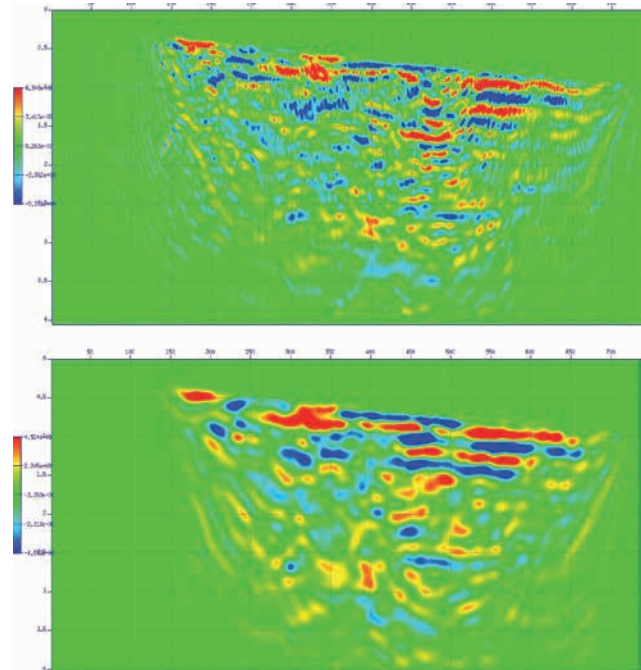


Figure 4 Gradient images masked and filtered (bottom) to improve the convergence of the objective function to the global minimum.

tion to improve convergence properties. The Hessian matrix is ignored in our solution and the gradient of the objective function is dominated by high wavenumbers (Sirgue, 2003). It requires some type of preconditioning of the gradient in

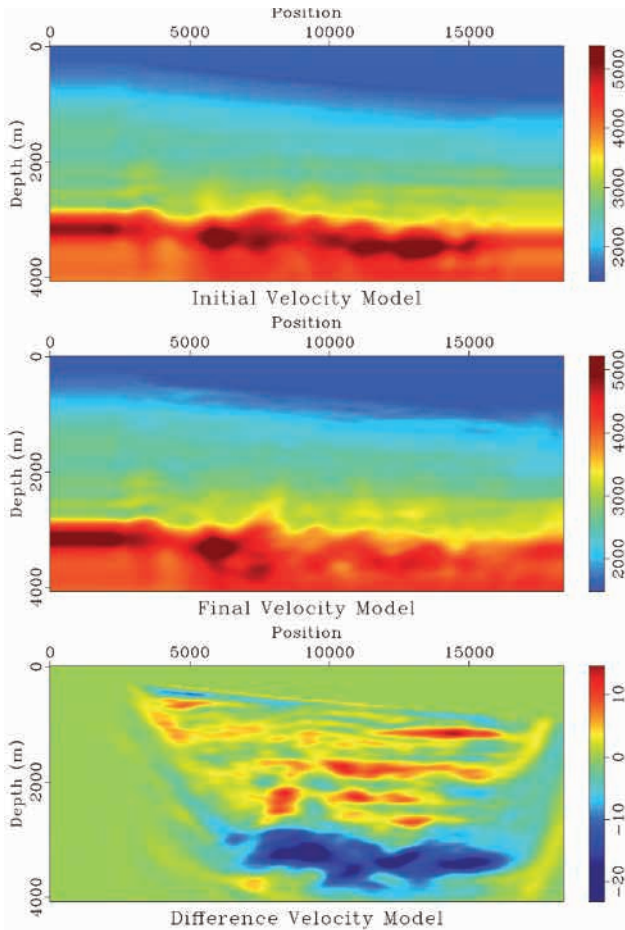


Figure 5 Initial velocity model (top), final velocity model (middle) and the percentage difference (bottom) showing the update after the waveform inversion.

order to ensure that the solution converges to the global minimum. There are several different types of preconditioning, but here the gradient was preconditioned by applying a simple wavenumber filter. A 2D low-pass elliptic/circular

filter is applied to the gradient in the wavenumber domain to remove the high wavenumber components (Figure 4). Each frequency group has its own optimised wavenumber filter, which, in practice, is obtained by interpreting the gradient after performing an inversion without a wavenumber filter. The idea is always to avoid higher wave numbers that are not expected in the gradient for that specific group of frequencies ($k_{max} = f_{max} / v_{min}$).

Results and QC

The previous sections discussed the waveform inversion parametrisation applied to the Campos Basin field data in order to obtain a more accurate and higher-resolution version of the P-wave velocity model.

Figure 5 shows the final waveform inversion results. The image includes the initial and final velocity models, and also the velocity difference (final – initial), which makes it easier to identify the update in the velocity model. Noticeable updates can be recognised throughout the entire model. Higher wavenumbers were locally introduced by the inversion in the shallow part of the model close to the sea floor. In addition, there is a strong update in the deepest part of the model, which decreases the velocity overall, where we have the high-velocity layers composed of carbonate/salt. Between 500 m and 2500 m the update mostly increased the velocities with a horizontal orientation that follows the main geological horizons of the area (Figure 7). The velocity difference emphasises the update in the final velocity model. The current inversion results have shown an improvement in the resolution and in the accuracy of the updated velocity model. The accuracy of the final velocity model was verified by conventional migrated images and common image gathers (CIGs) which can locally evaluate the velocity.

Figure 6 shows seismic images migrated with the initial and final velocity model, respectively. Both images were migrated using the preprocessed OBC dataset with RTM

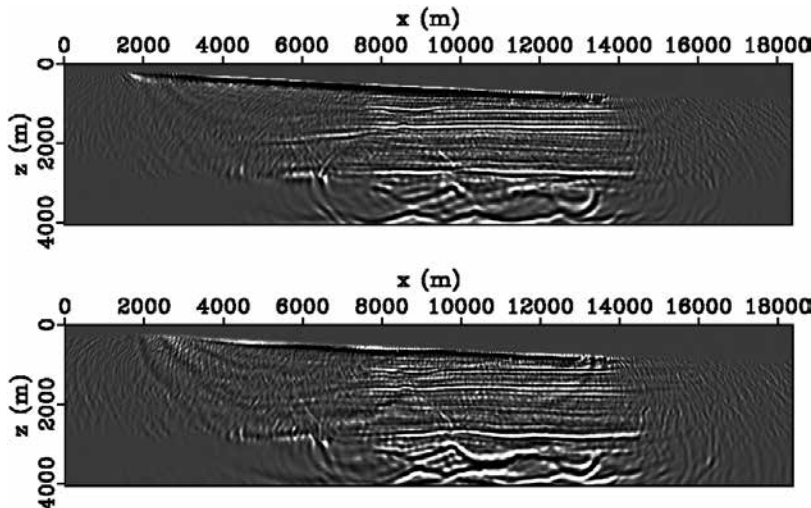


Figure 6 Seismic migrated images with original velocity model (top) and final velocity model (bottom).

Data Processing

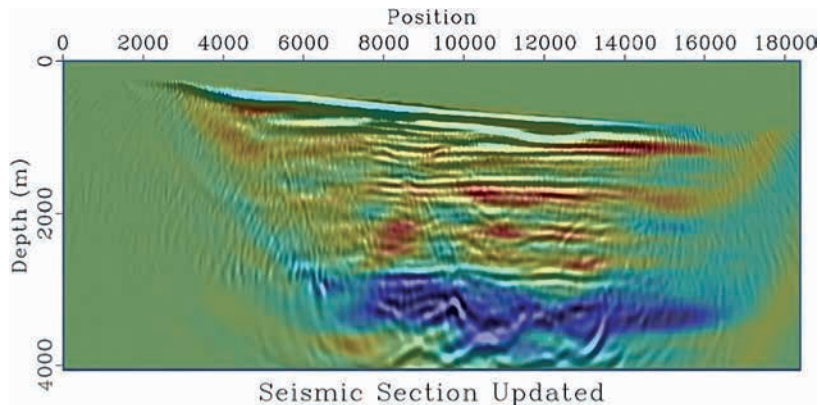


Figure 7 Migrated image overlaid with the final velocity difference. The larger velocity updates are related with the main horizons of the section.

migration algorithm (25 Hz peak frequency). Basically, the images show the same stacking quality, with good continuity and a focus on the main horizons in the shallow part of the line above approximately 2 km. However, the final seismic image was improved in the deeper part of the section below 2.2 km deep which includes the reservoir zone of interest. The overall decrease of the velocity at that depth enhanced the horizons' focus and continuity.

Figure 7 shows the final seismic image and the velocity difference overlaid, where the larger velocity updates are related with the main horizons of the section. In addition, the velocity update shows the decrease of the resolution with depth, mostly limited by the survey design (poor illumination), the diving waves approach and the maximum inverted frequency (15 Hz).

The improvements identified in the migrated image are confirmed by the CIGs. Figure 8 shows the CIGs computed for both velocity models, initial (top) and final (bottom), at sparse locations (8.0, 8.5, 9.0, 9.5, 10.0, 10.5, 11.0, 11.5, 12.0 and 12.5) km in the seismic section. The CIGs show information about the accuracy of the velocity and about angle illumination. The comparison between initial and final CIGs reveals that the final CIGs are cleaner. In the shallow part, above 2 km, the CIGs are similar, although in the deeper part there are two main recognisable events at approximately 2.7 km and 3.5 km, where the updated velocity flattened the events. It indicates that the velocity was corrected by the inversion, bringing greater accuracy to the velocity model. This accuracy is reflected in the seismic image through the focus and continuity of the horizons.

The largest update obtained in the deeper part of the model, which brought a huge improvement in the seismic image, is questionable. The ray tracing analysis shows that only a few rays travelled through the deeper part of the model, although the monochromatic wavefields show a larger interaction at that depth. The analysis and the strategy rely on the fact that the diving waves are the most important source of information to this update. However, the selection of the data used in the inversion (time damping - $\tau = 4$ s)

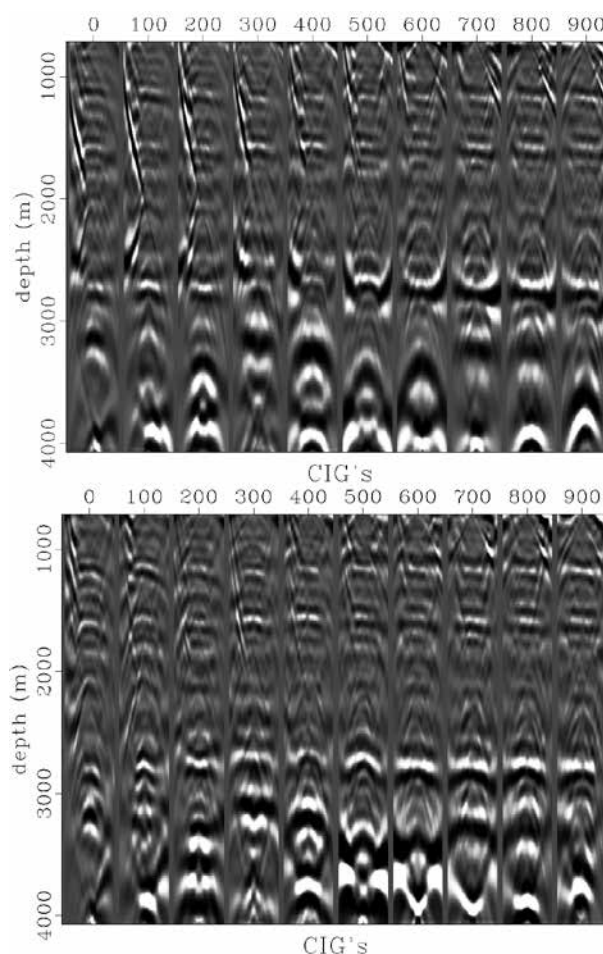


Figure 8 CIGs computed from wavefields of original (top) and final (bottom) velocity models at fixed positions (8.0, 8.5, 9.0, 9.5, 10.0, 10.5, 11.0, 11.5, 12.0 and 12.5) km.

might not be completely efficient to avoid reflections. The inversion could have used reflections to update the deeper part of the model, which can also be checked by the sensitivity kernel analysis.

Corroborated by the original Petrobras imaging processing that have included the VTI symmetry, and assuming

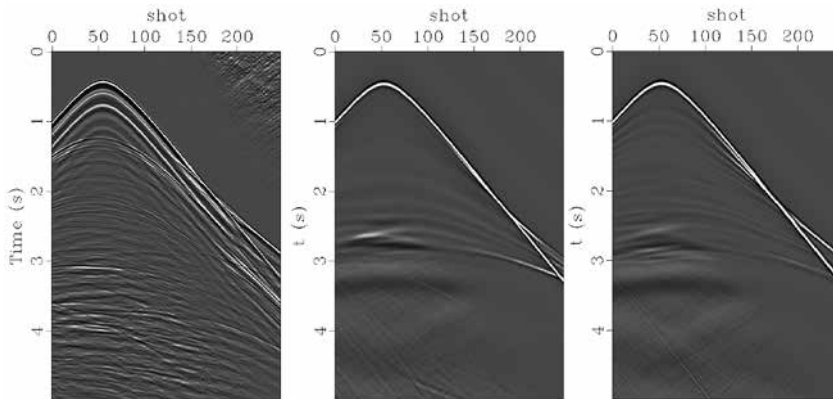


Figure 9 Comparison of observed shot, initial modelled shot and final modelled shot.

that the initial velocity model does not take it into account, the initial computed CIGs (Figure 8 (top)) show a seismic event at approximately 2.7 km deep with an anisotropic signature, called ‘hockey stick’. The seismic event is overcorrected, because of the lower vertical initial velocity compared with the correct velocity. In the final computed CIGs (Figure 8 (bottom)), the same seismic event appears more flattened, although it seems a bit undercorrected. Apparently, the inversion was more influenced by the horizontal velocity, because it is focused on diving waves, which is greater than the correct velocity obtained by VTI imaging processing.

The inversion results can also be checked by comparing shots from the observed and the modelled data, which are generated using the initial and final velocity models. Figure 9 shows this comparison, where it is possible to recognise if the final modelled shot is more similar to the observed shot. By the image, we recognise that the first breaks are well matched and there are some reflections brought by the inversion, when compared with the initial modelled shot. These reflections have really small amplitude and the final modelled shot is still far from representing the same complexity shown by the observed data. The inversion was able to bring some resolution, especially in the shallow part.

Conclusions and analysis

The waveform inversion results obtained for the OBC Campos dataset have shown improvements in the final velocity model. The final migrated image and the CIGs show that the final velocity model is more accurate, when the inversion corrected the background velocity generating more continuous and focused horizons at the depth of interest (reservoir depth). The new velocity model may be used in acoustic/elastic attributes inversion where it is crucial to incorporate more reliable velocity information, which will better constrain the results.

The limited resolution in the final results seems to be related to the parametrisation and the strategy used in the inversion. In order to improve the results, we could have

used the time damping relaxing approach which slowly incorporates more data into the inversions, i.e. reflections. In addition, we should have included in the later inversions a more robust objective function which combines the amplitude and phase residuals. This type of approach usually works well on synthetic data but requires an amplitude match procedure between observed and modelled data when applied to field data.

Acknowledgments

The authors would like to thank Petrobras for permission to publish these data results. We would also like to thank Prof Gerhard Pratt for providing the waveform tomography code to perform the inversions.

References

- Bednar, J.B., Shin, C. and Pyun, S. [2007] Comparison of waveform inversion, part 2: phase approach. *Geophysical Prospecting*, 55, 465–475.
- Pratt, R.G. [2013] Waveform tomography: theory and practice. 12th International Workshop on Controlled-Source Seismology, Extended Abstracts.
- Pratt, R.G. and Worthington, M.H. [1990] Inverse theory applied to multi-source crosshole tomography, part 1: Acoustic wave-equation method. *Geophysical Prospecting*, 38, 287–310.
- Pyun, S., Shin, C. and Bednar, J.B. [2007] Comparison of waveform inversion, part 3: amplitude approach. *Geophysical Prospecting*, 55, 477–485.
- Shin, C., Pyun, S. and Bednar, J.B. [2007] Comparison of waveform inversion, part 1: conventional wavefield vs logarithmic wavefield. *Geophysical Prospecting*, 55, 449–464.
- Sirgue, L. [2003] *Waveform inversion in the frequency domain for large offset seismic data*. Ph.D. Thesis, l'Université Paris XI.
- Sirgue, L. and Pratt, R.G. [2004] Efficient waveform inversion and imaging: A strategy for selecting temporal frequencies. *Geophysics*, 69, 231–248.
- Virieux, J. and Operto, S. [2009] An overview of full-waveform inversion in exploration geophysics. *Geophysics*, 74, WCC1–WCC26.
- Woodward, M.J. [1992] Wave-equation tomography. *Geophysics*, 57, 15–26.